

Preference of attractors in noisy multistable systems

Suso Kraut,¹ Ulrike Feudel,^{1,2} and Celso Grebogi^{1,2,3,4}

¹*Institut für Physik, Universität Potsdam, Postfach 601553, D-14415 Potsdam, Germany*

²*Institute for Plasma Research, University of Maryland, College Park, Maryland 20742*

³*Department of Mathematics, University of Maryland, College Park, Maryland 20742*

⁴*Institute for Physical Science and Technology, University of Maryland, College Park, Maryland 20742*

(Received 24 September 1998)

A model system exhibiting a large number of attractors is investigated under the influence of noise. Several methods for discriminating two qualitatively different regions of the noise intensity are presented, and the phenomenon of noise-induced preference of attractors is reported. Finally, the relevance of our findings for detection of multiple stable states of systems occurring in nature or in the laboratory is pointed out. [S1063-651X(99)01405-1]

PACS number(s): 05.45.-a, 05.40.Ca

I. INTRODUCTION

Typically, systems studied in the physical literature possess only a small number of coexisting attractors, which are the asymptotic states in the state space, corresponding to the long-term behavior. The long-term behavior becomes more involved if a system exhibits a larger number of coexisting attractors, because there exists a nontrivial relationship between these coexisting asymptotic states and their basins of attraction. The state which is finally approached depends crucially on the initial condition. This behavior, called multistability, is found in a variety of systems from different disciplines of science, like semiconductor physics [1–3], chemistry [4–7], neuroscience [8–10], and laser physics [11–13]. It was systematically investigated for the first time in Refs. [14] and [15] by performing experiments with a gas laser and numerical simulations of the Duffing oscillator, respectively. Usually in multistable systems the basins of attraction of different attractors are complexly interwoven, and separated by one or several chaotic saddles. The dimension of the basin boundaries is very close to the dimension of the state space. In addition, the introduction of noise to the dynamics of such a multistable system enhances even more the “complexity,” by introducing new dynamical behavior. The different basins of attraction, although they may already be fractal, change in a very intricate fashion. There exists a competition between the attractiveness toward regular motion in the neighborhood of an attractor and the jumping among the different attractors induced by the noise [16]. In fact, the noise kicks the orbit out of the open neighborhood of the attractor into the basin boundary. There the trajectory spends a certain amount of time until it reaches again the neighborhood of the same attractor or possibly another attractor. This process, in which the trajectory is in the neighborhood of the attractor or in the basin boundary region, keeps repeating. The length of these two characteristic phases of motion varies irregularly, and depends on the noise amplitude. This behavior is closely related to the so-called chaotic itinerancy [17–19], which has also been observed experimentally [20]. Recent studies on coupled oscillator systems with delay in the presence of noise [21] also reported phase transitions. This kind of multistability is also a

mechanism for memory storage and temporal pattern recognition [22,9,10]. A control study of systems with multiple coexisting attractors, and the steering of trajectories toward a desired attractor, was performed in Refs. [16,23]. Work that is closely related to the one presented here, but applied to coupled map systems, was carried out by Kaneko [24,25]. By treating high-dimensional systems, he found noise-induced selectivity for certain attractors. Similar results were also obtained in Ref. [26], investigating the Duffing oscillator and a circle map. However, in both works the implementation of noise is different from ours. This paper aims at a study of the influence of noise on highly multistable systems with a fractal basin boundary. It is organized as follows. In Sec. II, the model is introduced, and the relevant properties of the system are presented. Basic dynamical effects produced by noise are described. In particular, we present four methods for distinguishing between the dynamics dominated by attractor hopping and the one characterized by diffusion through the state space. Both phenomena are caused by the addition of noise, but yield qualitatively different dynamics. In Secs. III and IV the consequences of small and large noise, respectively, are discussed. As a main result, we argue that certain attractors are preferred due to the presence of small amounts of noise. Section V gives a summary.

II. MODEL

As our prototype model, we study the behavior of a periodically kicked mechanical rotor without gravity in the presence of noise. The motion of the rotor is usually modeled by differential equations. But taking into account that the kicks are only applied at certain discrete times $t = 0, T, 2T, \dots$, one can also model it by the following two-dimensional map:

$$x_{k+1} = x_k + y_k + \delta_x \pmod{2\pi}, \quad (1)$$

$$y_{k+1} = (1 - \nu) y_k + f_0 \sin(x_k + y_k) + \delta_y,$$

where x corresponds to the phase, y corresponds to the angular velocity, the parameter ν is the damping, and f_0 the

strength of the forcing. The terms δ_x and δ_y , where $\sqrt{\delta_x^2 + \delta_y^2} \leq \delta$, are the amplitude of the uniformly and independently distributed noise.

The noiseless system ($\delta_x = \delta_y = 0$) was studied in detail in Ref. [27]. There are two limiting cases. If the damping is maximal ($\nu = 1$), a one-dimensional circle map with zero phase shift is obtained. This map possesses only one attractor in large regions of the parameter space. For zero damping, the conservative limit, the Chirikov standard map results [28]. Islands of stability and chaotic motion coexist. The number of regular periodic states represented by the *KAM* islands is believed to be infinite. The two eigenvalues of these periodic orbits are complex conjugate, but their absolute values are exactly 1. The dynamics takes place on the torus $[0, 2\pi] \times [0, 2\pi]$. In particular, the family of period 1 orbits is given by $(x = \pi, y = m2\pi), m = 0, \pm 1, \dots$, which are, due to $\text{mod } 2\pi$, also in the y coordinate, all mapped onto the one with $m = 0$. Orbits of higher periods, so-called secondary islands, are grouped around these period 1 orbits, which correspond to primary islands. These islands around islands build a highly intricate hierarchy.

The introduction of dissipation changes the periodic orbits into sinks, since the absolute values of both eigenvalues are now slightly less than 1. The motion is now located on a cylinder $[0, 2\pi] \times \mathbb{R}$, and the period 1 periodic orbits for different m values become discernible. There is still some hierarchical organization of higher periodic orbits surrounding the period 1 orbits. However, the hierarchy known from the conservative case is disturbed by the dissipation. The number of periodic orbits is finite in the dissipative case, but can be made arbitrarily large by reducing the damping. By fixing the damping but varying the kick strength f_0 , a complex bifurcation diagram is obtained. Periodic orbits of low periods are generated through saddle-node bifurcations and they eventually undergo a period doubling cascade that ends in chaos. However, the chaotic intervals in, say, parameter f_0 are extremely small and hardly detectable numerically.

Let us fix the values of the parameters at $\nu = 0.02$, which is a rather small damping, and $f_0 = 3.5$ for the kick strength. For these parameter values, the periodic orbits of period 1 have not yet undergone the first period doubling. For this parameter set, there are no chaotic attractors, as they are in general rare in multistable systems with small dissipation [29,30]. We numerically find 111 coexisting periodic orbits for the noiseless case, the highest period being 32. They were found by iterating 10^6 initial conditions on a grid in part of the state space $[0, 2\pi] \times [-f_0/\nu, f_0/\nu]$. This part of the cylinder is the trapping region in state space, where all attractors are located. More than 99.9% of all found orbits are of periods 1 and 3, so all other periods do not play an important role in the following.

If noise is added to the dynamics, the trajectory alternates between almost periodic motion in the neighborhood of an attractor and chaotic motion in the basin boundary region in a very complex way. This behavior is illustrated in Fig. 1, where the x and y coordinates of the system are plotted for a large number of iterations and a noise level of $\delta = 0.1$. Clearly, there are almost periodic motions interspersed by random bursts. Although the periodic orbits are located in the state space in a hierarchical structure, there is not an apparent hierarchy of the jumping between the attractors,

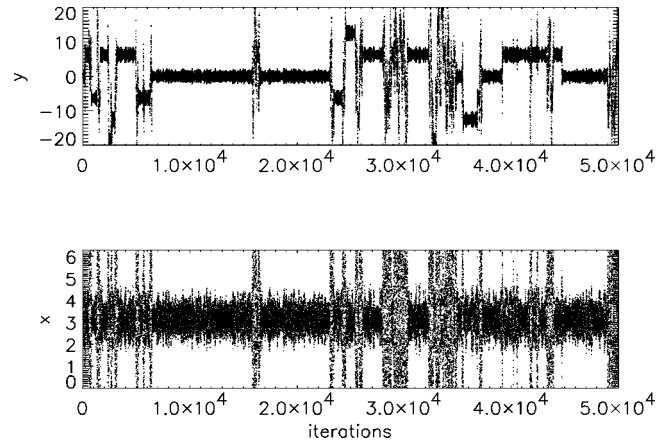


FIG. 1. Dynamics of the kicked single rotor under the influence of noise with intensity $\delta = 0.1$. Top: angular velocity y ; bottom: phase of the rotor x .

though the investigations on probability transition and entropy [16] suggest the existence of preferred transitions and of an itinerancy; however, this needs further investigations.

For the noisy dynamics, we ascertain that the motion is in the vicinity of a given periodic orbit in the following way. Every initial condition is checked after each k (~ 30) iterations, whether the orbit stays for a certain number of time steps l ($\sim 5 \times \text{period}$) close to the periodic orbit of the noiseless system, whereby closeness was specified by a maximum distance of about $j \approx 10\delta$. If these conditions are satisfied, the orbit is considered to be trapped in the neighborhood of the specific attractor. However, the exact numerical values of these choices (k, l, j) do not possess any crucial meaning, and changing them by moderate amounts yields similar results. Using these criteria to ensure that the orbit is in the vicinity of a periodic attractor, we finally investigate how the basins of attraction for different attractors change as we vary the noise level. For this purpose, we stop iterating the trajectory as soon as it reaches the neighborhood j of an attractor for the first time. Hereby we disregard the fact that the trajectory can be kicked out of this neighborhood by the noise at a later time. In Fig. 2 we illustrate the effect of noise by a

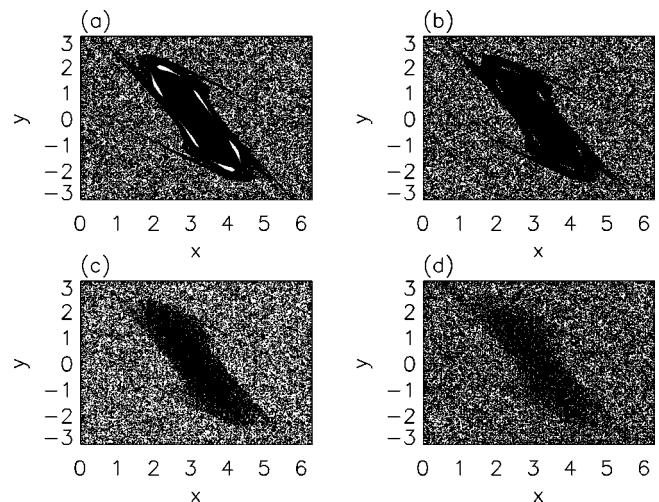


FIG. 2. Basin of the fixed point $(x = \pi, y = 0)$ for increasing noise levels. (a) $\delta = 0$. (b) $\delta = 0.01$. (c) $\delta = 0.1$. (d) $\delta = 0.3$.

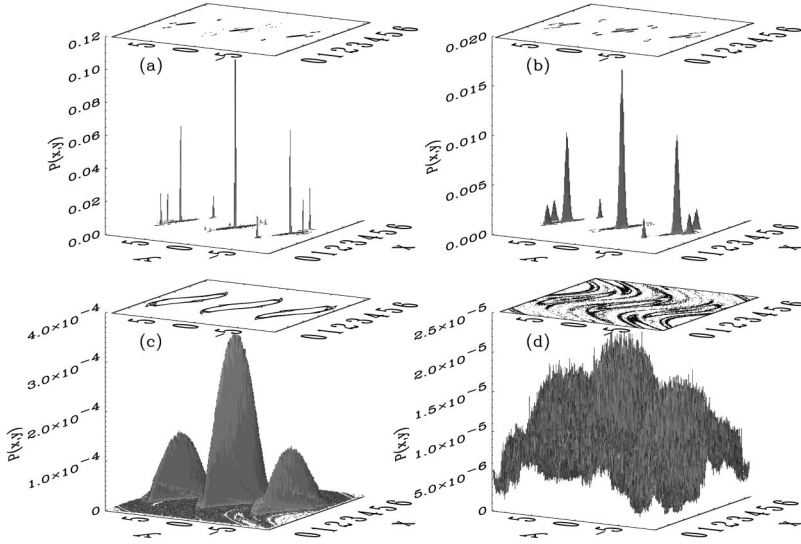


FIG. 3. Probability density $P(x,y)$ in the rectangle $[0,2\pi] \times [-3\pi,3\pi]$ for increasing noise levels. The same noise levels as in Fig. 2 are used. (a) $\delta=0.001$. (b) $\delta=0.01$. (c) $\delta=0.1$. (d) $\delta=0.3$. On the top of each figure, a contour plot of a certain probability density $P_c(x,y)$ is shown. $P_c(x,y)$ has the values (a) 2.4×10^{-4} , (b) 2.5×10^{-5} , (c) 2.3×10^{-4} , and (d) 2.2×10^{-5} .

series of pictures of the basins of attraction for the main fixed point ($x=\pi, y=0$) for different noise amplitudes. For a tiny noise amplitude ($\delta=0.01$) a great similarity with the noiseless basin is seen, including the two embedded open neighborhoods of the two period 3 attractors. The fine structure becomes increasingly blurred with increasing noise intensity, e.g., ($\delta=0.1$). For a large noise level ($\delta=0.3$) the basic structure is still present, but it starts to become washed out. For each initial condition different noise realizations are used to create the picture of the basin of attraction. The size of the basins and the qualitative structure remain the same under other noise realizations. Let us now use a probabilistic approach which is often employed in the study of noisy systems. Instead of focusing on individual trajectories, we focus on the probability density depending on the state variables x and y . Similar conclusions to these obtained for single trajectories are drawn from the behavior of the probability density, as shown in Fig. 3. In this figure we use 1000 initial conditions, randomly distributed in the rectangle $[0,2\pi] \times [-3\pi,3\pi]$, and we iterate each one for 10 000 steps. This region of the state space is covered with a 300×300 grid, and every visit of a grid cell is counted, thus creating a numerically generated probability density. The same noise amplitudes as used in Fig. 2 are also chosen in Fig. 3, except for the substitution $\delta=0.001$ for $\delta=0$ to avoid δ -peaked distribution. As can be seen, the peaks of the period 1 and 3 orbits become increasingly broad, until almost no structure is present anymore, indicating the predominance of diffusion due to the noise. Figures 2 and 3 also confirm our numerical procedure. For instance, they show that the period 3 orbits are still present in the noisy dynamics as well as in the long-term behavior as approximated by the first visit to a periodic orbit. Both figure sequences, Figs. 2 and 3, illustrate the process of loss of fine-scale structure of the basins of attraction with increasing noise intensity. As we will describe next, this process can be characterized as a transition from small to large noise levels with different consequences for the dynamics of the system.

III. METHODS

The characteristic change in the role of the noise at a noise level of about $0.05 < \delta < 0.1$ is examined by four dif-

ferent methods. First, we consider the Lyapunov exponent of a trajectory, as depicted in Fig. 4. In the noiseless case, only periodic motion occurs as long-term behavior, yielding a negative Lyapunov exponent. By contrast, the introduction of noise yields a positive Lyapunov exponent. It becomes significantly positive for $\delta \approx 0.047$. This value is determined by using finite-time Lyapunov exponents $\lambda_T = (1/T) \sum_{i=1}^T \ln |(df/dx)_i|$. Here T is the length of the time interval, and $(df/dx)_i$ is the Jacobian of the map for each time step i . When we compute those λ_T for an ensemble of L ($L \gg 1$) trajectories at a given time interval T , we obtain a set of positive finite-time exponents λ_i^+ , and a set of negative ones λ_i^- corresponding to chaotic or almost periodic motion, respectively. Using this distribution of finite-time Lyapunov exponents, we estimate the noise intensity for which the asymptotic Lyapunov exponent λ becomes positive. This noise value satisfies

$$\lambda(\delta) = \frac{1}{L} \left(\sum_{i=1}^M \lambda_i^+ + \sum_{i=1}^N \lambda_i^- \right) \approx 0. \quad (2)$$

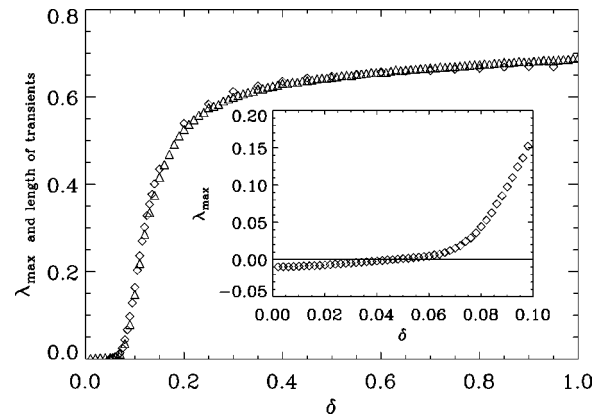


FIG. 4. Maximum Lyapunov exponent (\diamond) and average length of transients (\triangle) vs noise level. For each noise intensity, λ_{\max} and the length of the transients are calculated by averaging over 50 trajectories with 10^6 iterations each. The inset shows the crossing of the Lyapunov exponent curve through zero. This takes place at $\delta \approx 0.047$ with a slope of 0.27.

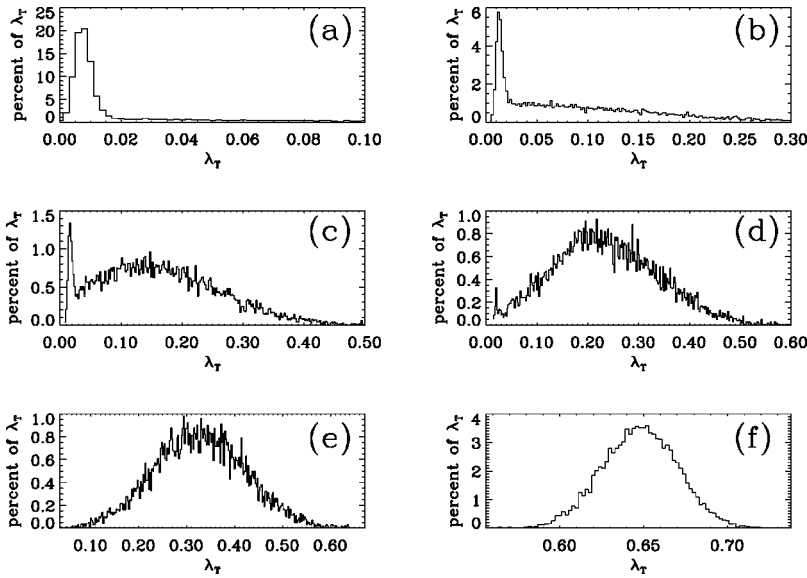


FIG. 5. Histograms of finite-time Lyapunov exponents for different noise levels. The trajectory length is 5000. Altogether 10 000 Lyapunov exponent values are computed for each picture, using 50 trajectories. The bin size is 0.002. (a) $\delta=0.075$. (b) $\delta=0.09$. (c) $\delta=0.1$. (d) $\delta=0.11$. (e) $\delta=0.125$. (f) $\delta=0.5$.

Here L is the total number of trajectories, while $M(N)$ is the number of trajectories yielding positive (negative) finite-time Lyapunov exponents λ_i^+ (λ_i^-), respectively. This effect is an example of the so called “noise-induced chaos,” first observed in the logistic map [31,32], and subsequently in a variety of systems, like Josephson junctions [33], superconducting quantum interference devices [34], and the Kramers oscillator [35]. In Fig. 4, we also plot the average length of the chaotic bursts between regular motions in the neighborhood of attractors (cf. Fig 1). We measure this length of the chaotic transients by splitting 50 trajectories of 10^6 iterations into blocks of five iterations, and checking in each of these blocks whether the motion is in the vicinity of an attractor or is chaotic. The functional form of these averaged lengths of the chaotic bursts very much resembles the behavior of the Lyapunov exponents. This has to be expected, according to Eq. (2), since the bursting corresponds to a positive Lyapunov exponent, while periodic motion corresponds to a negative exponent. Thus for higher noise amplitudes the overall motion is chaotic, albeit almost periodic phases are interspersed into the dynamics. This indicates that the phases of jumping in the intertwined basin boundary, consisting of chaotic saddles, gain increasingly more weight.

The second method consists of searching for the minimal noise level to escape from an attractor into the basin boundary region. We require that noise should be able to remove the trajectory from every neighborhood of a periodic orbit. Though the noise level depends on the size of the neighborhood as well as the eigenvalues of the periodic orbit, as we will argue later, we consider the largest basin of attraction ($x=\pi, y=0$). We increase the noise intensity gradually, and look for the minimum value of δ at which the trajectory leaves the open neighborhood of the attractor for the first time. By averaging over 200 trajectories with different noise realizations and a very large number of iterations (5×10^7), this results in $\delta \approx 0.06$. Below this value, the trajectory, although being contaminated by noise, may be trapped in the open neighborhood of this attractor *forever*. Above this value the trajectory diffuses freely over the whole state space, staying only a *finite time* in the neighborhood of *any* attractor.

A third method is considered by looking at the distribu-

tion of finite-time Lyapunov exponents. These distributions are approximated by histograms of the finite-time exponents λ_T . They are computed for $T=5000$ and using 50 time series of length 1 000 000. This yields 10 000 Lyapunov exponent values which are enough for a sufficiently good statistics. Smaller time intervals T do not give good results, since the eigenvalues are complex and, by this fact, spurious peaks appear in the histograms, due to the rotation of the eigenvectors. For the noiseless system, the motion is attractive, and hence the finite-time Lyapunov exponents are negative, peaking about the maximum Lyapunov exponent, whose numerical value is $\lambda_{\max} \approx -0.01$. As the noise intensity increases, the peak is shifted towards higher values of λ_{\max} and starts to flatten out. At a noise level of $\delta=0.075$, there is no longer any negative Lyapunov exponent, and a second peak at a higher value begins to develop; see Fig. 5(a). This second peak becomes increasingly dominant and develops into a Gaussian distribution, displayed in Figs. 5(b) and 5(c). For $\delta=0.125$ [Fig. 5(e)] the Gaussian part is fully developed, and the peak associated with the periodic motion is no longer visible. Increasing the noise further yields a single Gaussian distribution [Fig. 5(f)], whose mean is in accordance to the maximal Lyapunov exponent of Fig. 4. The peak corresponding to the periodic motion has disappeared completely. This transition thus takes place at around $0.08 < \delta < 0.12$.

The fourth method is provided by considering the Fourier spectrum of a noisy time series. The investigation of the spectra is motivated by a claim of Arecchi and co-workers [36,37], who stated that a multistable system with a fractal basin boundary disturbed by noise in such a way that attractor hopping occurs exhibits a $1/f^\alpha$ spectrum. This claim is validated by our Figs. 6–8. Only in the case of an intermediate noise level of $\delta=0.085$ can the nontrivial low frequency part of the spectrum be observed, which is well described by $S(f) \sim 1/f^\alpha$ and $\alpha \approx 1$ (Fig. 7, solid line). In contrast, if the noise is too weak for exiting the attractor (Fig. 6) or too large for staying close to an attractor for a longer time (Fig. 8), the spectrum is similar to that of Brownian motion. Therefore, it can be very well fitted by a Lorentzian with a flat (white) low frequency part and a $1/f^2$ high frequency part. Hence this is a criterion for distinguishing among different noise levels.

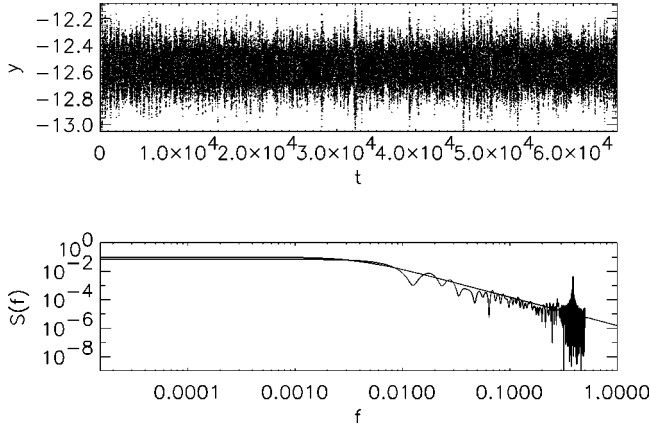


FIG. 6. Time series of the angular velocity y (top) and the corresponding fast Fourier transform (FFT) spectrum $S(f)$ (bottom) for a noise level of $\delta=0.01$ and a length of $2^{16}=65\,536$. The noise is not strong enough to kick the orbit out of one of the attractors; therefore, no hopping takes place and the whole spectrum follows a Lorentzian.

Altogether there exists a qualitative change in the systems dynamics around a certain noise level of $0.05 < \delta < 0.1$. Below this transition the dynamics of the system is characterized by a motion consisting of regular phases in the neighborhood of attractors and chaotic phases on the basin boundary, establishing the hopping between attractors. Beyond the crossover, noise induced diffusion over the state space is the dominating process. Because of this phenomenology, we split the treatment into small and large noise effects.

IV. EFFECTS OF SMALL NOISE

As pointed out in Sec. III increasing noise results in a loss of fine structure in the basins of attraction. The small basins seem to be more sensitive than the large ones. To explore this effect in more detail, we investigate the influence of noise on the size of the basins. In Fig. 9, the number of initial conditions terminating (according to our numerical procedure)

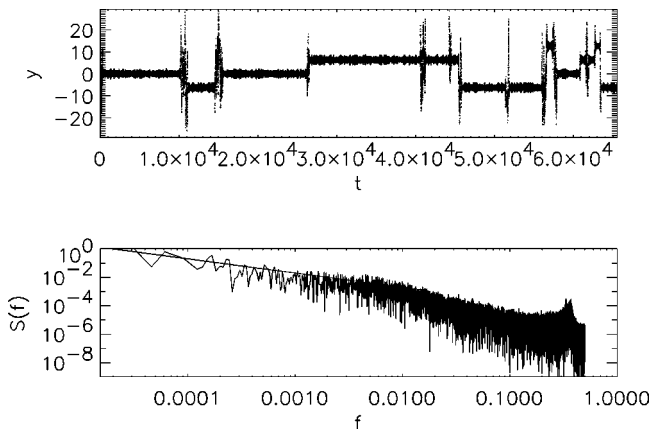


FIG. 7. Time series of the angular velocity y (top) and the corresponding FFT spectrum $S(f)$ (bottom) for a noise level of $\delta=0.085$. Here a competition between hopping and remaining in an attractor exists, which results in the low frequency part of the spectrum, which can be fitted by $S(f) \sim 1/f^\alpha$ for $f < 0.005$ (solid line).

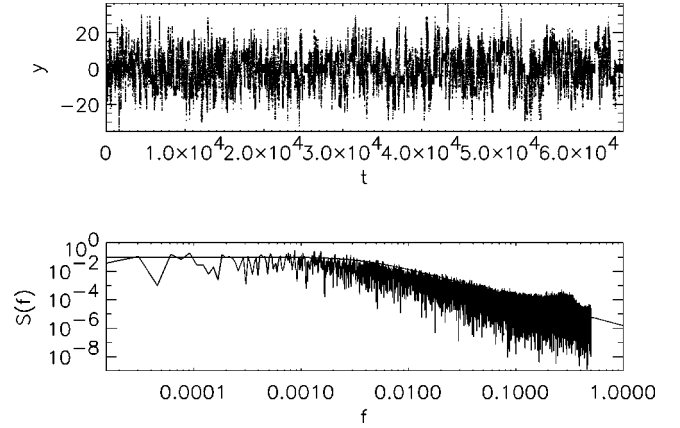


FIG. 8. Time series of the angular velocity y (top) and the corresponding FFT spectrum $S(f)$ (bottom) for a noise level of $\delta=0.2$. For such a high noise intensity diffusive motion dominates, and the trajectory does not remain for an appreciable length of time in the neighborhood of an attractor. The entire spectrum is again very well fitted by a Lorentzian.

on the period 1 orbits with different m is plotted against the noise level. It can clearly be seen that the curves for different m all possess roughly the same features, namely, there is an increase up to a maximum value, followed by an exponential decrease taking place at lower noise intensity for higher m values. The relevant region for this behavior stretches to about $\delta=0.08$, confirming once again the threshold for the dynamics dominated by attractor hopping. As stated above, the decay after the maximum value is well fitted by an exponential. The determination of the slopes of these exponentials reveals that the slopes also yield roughly an exponential scaling. Furthermore, the starting points of the decrease in the dependence of m yields an exponential law as well.

All these features are even more robust by considering multiplicative noise. Generally, multiplicative noise is applied by perturbing the form of the function. In our case this amounts to altering the kick strength f_0 , and we do this by introducing a noise term via $f_0 \mapsto f_0 + \delta$ into the second of Eqs. (1). This results in the additive term $\delta \sin(x_k + y_k)$ acting

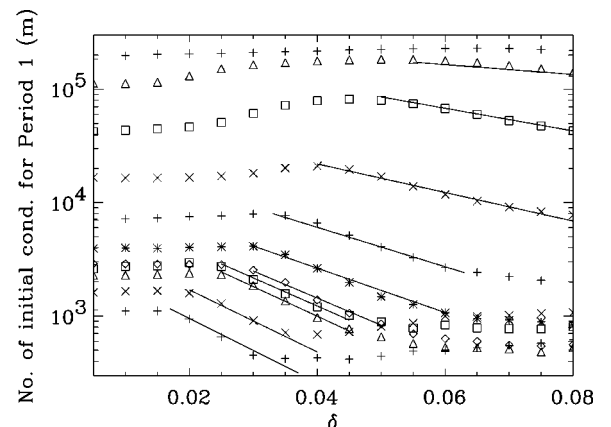


FIG. 9. Number of initial conditions converging to period 1 attractors with increasing m from top ($m=0$) to bottom ($m=10$). Because of the symmetry $m=+k$ and $m=-k$ are averaged. Altogether 10^6 initial conditions are iterated.

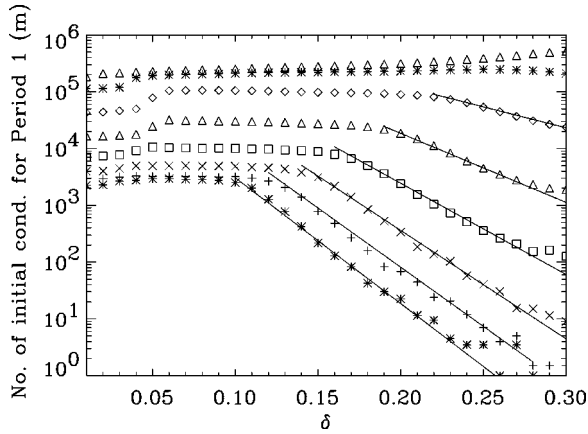


FIG. 10. Same as in Fig. 9 for $m=0$ (top) to $m=7$ (bottom), but with multiplicative noise.

on the angular velocity only. The strength of the resulting noise depends then on the present location of the trajectory and it is always $\leq \delta$. Figure 10 exhibits the corresponding information to Fig. 9. The expected behavior occurs at higher noise intensities, and is due to the effective reduction of the influence of the noise by multiplying δ with the sin term. In particular, for the fixed points $y=2\pi m$, x is close to π , and thus the sin term is very small. For multiplicative noise the exponential decay is even more pronounced. Again the slopes and the snap-off points scale exponentially.

For higher noise strength the attractors with small basins lose part of their basins, while the ones with an already large basin are preferred. Thus the fine structure of the system is washed out due to the noise. This leads to an important consequence for the behavior of multistable systems. Even if the number of coexisting attractors is very high in a deterministic system, one observes only few of those attractors in the presence of noise. The behavior is dominated by a few preferred attractors, while the majority of them “disappears.” Since in nature or in experimental systems noise is always inevitable, one can expect that only a tiny number of asymptotic states can be “measured” while the majority remains “hidden.” On the other hand, if the noise level corresponds to the maxima in Fig. 9, the opposite effects occurs: that is, attractors with a small basin gain more initial conditions, and the basins of many of them become even larger as compared with the no noise basin. This is especially true in the case of the period 3 attractors. This remarkable effect may be explained by the fact that the eigenvalues of the period 3 orbits are slightly smaller than those of the period 1 fixed points. Additionally, the open neighborhoods of the period 3 attractors are located within the open neighborhood of the fixed points; see Fig. 2. For $f_0=4$, this is not the case, and the effect cannot be observed. This effect of a noise-induced increase in the size of the basin of attraction has been also observed in coupled map lattices [24,25] and a bistable system [26]. The bistable system exhibits two periodic orbits with a fractal basin boundary, and the condition that one basin has to be “inside” the other one is trivially fulfilled, while in the coupled map lattice case the attractors possess riddled basins of attraction. This riddling also provides the seemingly necessary condition for the appearance of noise-induced selectivity of certain attractors.

To obtain a better understanding for the effect of noise in

TABLE I. The modulus of the eigenvalues, the minimal noise intensity necessary for escape, and the “potential” from Kramers law.

| m | $ \lambda $ | $\min(\delta_{\text{escape}})$ | U |
|-----|-------------|--------------------------------|--------|
| 0 | 0.98994952 | 0.061 | 0.034 |
| 1 | 0.98994952 | 0.05 | 0.022 |
| 2 | 0.98994952 | 0.041 | 0.015 |
| 3 | 0.98994952 | 0.031 | 0.0086 |
| 4 | 0.98994952 | 0.026 | 0.0065 |
| 5 | 0.98994952 | 0.021 | 0.0038 |

our nonlinear model, we study a very simple linear system with noise, given by

$$x_{k+1} = \alpha x_k + \delta_x, \quad (3)$$

$$y_{k+1} = \beta y_k + \delta_y,$$

where α and β are less than 1. All nonlinearities and couplings from the original model are absent here. A stable fixed point exists at $(x=0, y=0)$, from which the orbit cannot escape. The maximum distance $D = \max(|x|, |y|)$ of the orbit from the fixed point is given by

$$D = \sum_{i=0}^{\infty} \max(|\alpha|, |\beta|)^i \delta = \frac{\delta}{1 - \max(|\alpha|, |\beta|)}. \quad (4)$$

In our nonlinear system, however, the norm of the maximal eigenvalues for the period 1 fixed points $|\lambda|$ is exactly identical for all m , while the minimum noise intensity $\min(\delta_{\text{escape}})$, for which the trajectories leave the attractors for the first time, decreases with m , as shown in Table I. This result underlines the importance of the nonlinearities in this model. Furthermore, it is important to note that the eigenvalues are close to the stability threshold $|\lambda|=1$. For noise intensities larger than the minimum noise intensity $\min(\delta_{\text{escape}})$, the trajectories leave eventually the open neighborhood of the attractor. The escape times differ for each noise realization yielding an exponential distribution $P(\tau) \sim \gamma \exp[-\gamma(\tau - \tau_{\text{opt}})]$, as shown in Fig. 11 for $m=0$. In principle, by using the relation $\langle \tau - \tau_{\text{opt}} \rangle = 1/\gamma$, the optimal es-

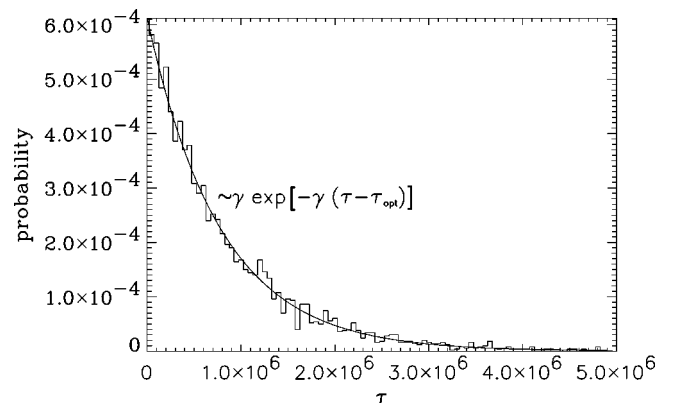


FIG. 11. Distribution of escape times $\langle \tau \rangle$ for the fixed point $m=0$ (the bin size is 50 000).

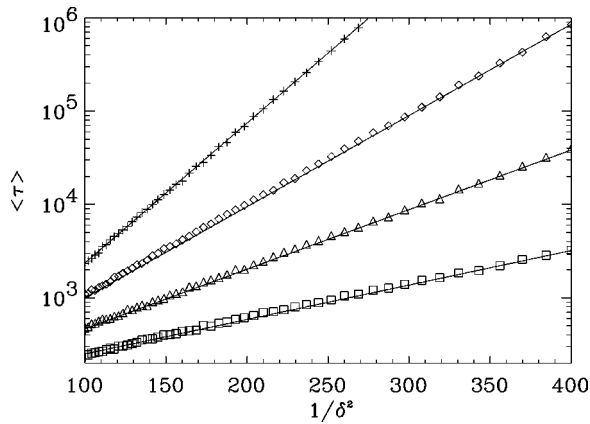


FIG. 12. Escape times $\langle \tau \rangle$ vs $1/\delta^2$ for different fixed points in a semilogarithmic plot ($m=0,1,2$, and 3 from top to bottom). The slopes U correspond to the potential values of Kramers law $\langle \tau(\delta) \rangle \sim \exp(U/\delta^2)$.

cape time can be determined. However, we numerically obtain only the approximate result $\tau_{\text{opt}} \leq 300$.

Let us now look at the scaling of the mean escape times with increasing noise level. In Fig. 12 the mean escape times for different m values are depicted. They follow Kramers law $\langle \tau(\delta) \rangle \sim \exp(U/\delta^2)$ very well, which is far from trivial in cases where, like here, no potential U exists [38,39]. The ratio $U/\min(\delta_{\text{escape}})^2$ is roughly constant, which suggests that, in first order, the stability of each attractor can be approximated by a parabolic potential.

V. LARGE NOISE

When the noise intensity is increased over the transition region of about $0.05 < \delta < 0.1$, the stochasticity is the dominant part of the dynamics. This behavior is reflected in the autocorrelation function $C_{xx}(\tau) := (1/T) \sum_{t=0}^T (x_t - \langle x_t \rangle)(x_{t+\tau} - \langle x_{t+\tau} \rangle)$ of a noisy trajectory. It decreases exponentially with an exponent sharply rising at about $\delta \sim 0.09$, the qualitative behavior following roughly the curve of the maximal Lyapunov exponent (Fig. 4). However it is still different from a pure random process, which is characterized by no

autocorrelation. This fact is also apparent in Fig. 2(d). Although much of the fine structure of the basin is blurred by the noise, it is still present. To classify this effect with measures of complexity is a current topic of our investigations.

VI. DISCUSSION

In summary, we have investigated the influence of noise on a multiattractor system. In this paper, we exclusively use independent and uniformly distributed noise. However, the main results are also obtained working with Gaussian noise, which does not seem to introduce any significant difference, except for the fact that for each attractor a specific and finite amount of noise is necessary to “kick” the trajectory out of its open neighborhood. The treatment of the behavior of the system in the presence of noise is split into two regions of noise intensity. The existence of a crossover region separating them is demonstrated by four criteria. Although the exact numerical values resulting from these different methods do not agree completely, they yield a coherent and conclusive picture. For low noise, attractor hopping is the dominant part of the dynamics, and the interesting phenomenon of noise-induced preference of certain attractors is observed. Above the crossover region, mainly diffusive motion exists, and the fine-scale dynamics is not relevant anymore. By and large, the investigation sheds some light on the measurement of multistable systems in nature, where in spite of the large number of attractors only few are *de facto* detected. Consequently, the observation of only a small number of stable states in physical systems may not necessarily lead to the conclusion that the system does not possess more of them. There may still be a larger number of attractors, which the experimenter is not aware of: they are just hidden by the inherent noise.

ACKNOWLEDGMENTS

We would like to thank H. Kantz, A. Pikovsky, and U. Schwarz for valuable discussions. U.F. thanks the University of Maryland for their hospitality. This work was supported by the Deutsche Forschungsgemeinschaft and a NSF/CNPq joint grant.

-
- [1] F. Prengel, A. Wacker, and E. Schöll, Phys. Rev. B **50**, 1705 (1994).
 [2] J. Kastrop, H. T. Grahn, and E. Schöll, Appl. Phys. Lett. **65**, 1808 (1994).
 [3] B. Sun Ning, Phys. Rev. B **51**, 11 221 (1995).
 [4] P. Marmillot, M. Kaufmann, and J.-F. Hervagault, J. Chem. Phys. **95**, 1206 (1991).
 [5] K. L. C. Hunt, J. Kottalam, M. D. Hatlee, and J. Ross, J. Chem. Phys. **96**, 7019 (1992).
 [6] J. Liu and S. K. Scott, Dyn. Stability Syst. **8**, 273 (1993).
 [7] R. S. MacKay and J.-A. Sepulchre, Physica D **82**, 243 (1995).
 [8] C. C. Canavier, D. A. Baxter, J. W. Clark, and J. H. Byrne, J. Neurophysiol. **69**, 2252 (1993).
 [9] J. Foss, A. Longtin, B. Mensour, and J. Milton, Phys. Rev. Lett. **76**, 708 (1996).
 [10] J. Foss, F. Moss, and J. Milton, Phys. Rev. E **55**, 4536 (1997).
 [11] M. Brambilla, F. Battipede, L. A. Lugiato, V. Penna, F. Prati, C. Tamm, and C. O. Weiss, Phys. Rev. A **43**, 5090 (1991).
 [12] M. Brambilla, L. A. Lugiato, V. Penna, F. Prati, C. Tamm, and C. O. Weiss, Phys. Rev. A **43**, 5114 (1991).
 [13] Z. Wang, W. Guo, and S. Zheng, Phys. Rev. A **46**, 7235 (1992).
 [14] F. T. Arecchi, R. Meucci, G. Puccioni, and J. Tredicce, Phys. Rev. Lett. **49**, 1217 (1982).
 [15] F. T. Arecchi, R. Badii, and A. Politi, Phys. Rev. A **32**, 402 (1985).
 [16] L. Poon and C. Grebogi, Phys. Rev. Lett. **75**, 4023 (1995).
 [17] K. Ikeda, K. Matsumoto, and K. Otsuka, Prog. Theor. Phys. Suppl. **99**, 295 (1989).
 [18] K. Tsuda, World Futures **32**, 167 (1991).

- [19] K. Kaneko, *Physica D* **41**, 38 (1990).
- [20] F. T. Arecchi, G. Giacomelli, P. L. Ramazza, and S. Residori, *Phys. Rev. Lett.* **65**, 2531 (1990).
- [21] S. Kim, S. H. Park, and C. S. Ryu, *Phys. Rev. Lett.* **78**, 1616 (1997).
- [22] S. Kim, S. H. Park, and C. S. Ryu, *Phys. Rev. Lett.* **79**, 2911 (1997).
- [23] Y.-C. Lai, *Phys. Lett. A* **221**, 375 (1996).
- [24] K. Kaneko, *Phys. Rev. Lett.* **78**, 2736 (1997).
- [25] K. Kaneko, *Physica D* **124**, 322 (1998).
- [26] W. Yang, M. Ding, and H. Gang, *Phys. Rev. Lett.* **74**, 3955 (1995).
- [27] U. Feudel, C. Grebogi, B. R. Hunt, and J. A. Yorke, *Phys. Rev. E* **54**, 71 (1996).
- [28] B. V. Chirikov, *Phys. Rep.* **52**, 265 (1979).
- [29] U. Feudel and C. Grebogi, *Chaos* **7**, 597 (1997).
- [30] U. Feudel and C. Grebogi (unpublished).
- [31] G. Meyer-Kress and H. Haken, *J. Stat. Phys.* **26**, 149 (1981).
- [32] J. P. Crutchfield, J. D. Farmer, and B. A. Huberman, *Phys. Rep.* **92**, 45 (1982).
- [33] M. Iansiti, Q. Hu, R. M. Westervelt, and M. Tinkham, *Phys. Rev. Lett.* **55**, 746 (1985).
- [34] A. R. Bulsara and E. W. Jacobs, *Phys. Rev. A* **42**, 4614 (1990).
- [35] L. Schimansky-Geier and H. Herzog, *J. Stat. Phys.* **70**, 141 (1993).
- [36] F. T. Arecchi and F. Lisi, *Phys. Rev. Lett.* **49**, 94 (1982).
- [37] F. T. Arecchi and A. Califano, *Europhys. Lett.* **3**, 5 (1987).
- [38] P. Beale, *Phys. Rev. A* **40**, 3998 (1989).
- [39] P. Grassberger, *J. Phys. A* **22**, 3283 (1989).